ScienceDirect
IFAC Papers Online
CONFERENCE PAPER ARCHIVE
IFAC-PapersOnLine 48-9 (2015) 251–256

Model Predictive Control for Spacecraft Rendezvous in Elliptical Orbits with On/Off Thrusters ⋆

Rafael Vazquez * **Francisco Gavilan** * **Eduardo F. Camacho** **

* *Departamento de Ingeniería Aeroespacial*
** *Departamento de Ingeniería de Sistemas y Automática*
Universidad de Sevilla, Camino de los Descubrimientos s/n, 41092, Sevilla, Spain (rvazquez1@us.es, fgavilan@us.es, eduardo@esi.us.es)

Abstract: In previous works, the authors have developed a trajectory planning algorithm for spacecraft rendezvous which computed optimal Pulse-Width Modulated (PWM) control signals, for circular and eccentric Keplerian orbits. The algorithm is initialized by solving the impulsive problem first and then, using explicit linearization and linear programming, the solution is refined until a (possibly local) optimal value is reached. However, trajectory planning cannot take into account orbital perturbations, disturbances or model errors. To overcome these issues, in this paper we develop a Model Predictive Control (MPC) algorithm based on the open-loop PWM planner and test it for elliptical target orbits with arbitrary eccentricity (using the linear time-varying Tschauner-Hempel model). The MPC is initialized by first solving the open-loop problem with the PWM trajectory planning algorithm. After that, at each time step, our MPC saves time recomputing the trajectory by applying the iterative linearization scheme of the trajectory planning algorithm to the solution obtained in the previous time step. The efficacy of the method is shown in a simulation study where it is compared to MPC computed used an impulsive-only approach.

Keywords: Spacecraft autonomy, Space robotics, Pulse-width modulation, Trajectory planning, Optimal trajectory, Linearization.

1. INTRODUCTION

Technology enabling simple autonomous spacecraft rendezvous and docking is becoming a growing field as access to space continues increasing. The field has become very active in recent years, with an increasingly growing literature. Among others, approaches based on trajectory planning and optimization (Breger and How (2008); Arzelier et al. (2013, 2011)) and predictive control (Richards and How (2003); Rossi and Lovera (2002); Asawa et al. (2006); Gavilan et al. (2009, 2012); Larsson et al. (2006); Hartley et al. (2012); Leomanni et al. (2014)) are emerging.

Classically, in these approaches the problem of rendezvous is modeled by using impulsive maneuvers; one computes a sequence of (possibly optimal) impulses (usually referred to as ΔV's) to achieve rendezvous. Other methods allow the control signal (thrust) to take any value inside an allowed range. This type of control signal is usually referred to as Pulse-Amplitude Modulated (PAM).

However, neither impulsive actuation nor PAM actuation capture with precision the behavior of real spacecraft thrusters. A more realistic model has to take into account that, typically, thrusters are ON-OFF actuators, i.e., the thrusters are not able to produce arbitrary forces, but instead can only be switched on (producing the maximum amount of force) or off (producing no force). These switching times are the only signals that can be controlled. This type of control signal is usually referred to as Pulse-Width Modulated (PWM). Trajectory planning in the rendezvous problem with PWM actuation poses a challenge because the system becomes nonlinear in the switching times.

Recently, Vazquez et al. (2011, 2014) introduced a trajectory planning algorithm algorithm for spacecraft rendezvous that was able to incorporate PWM control signals. The former considered the linear time-invariant Clohessy-Wiltshire model (target orbiting in a *circular* Keplerian orbit, see Clohessy and Wiltshire (1960)). The latter extended the approach to *elliptical* target orbits by using the linear time-varying Tschauner-Hempel model (see Tschauner and Hempel (1965)). Both methods start from an initial guess computed by solving an optimal linear program with PAM or impulsive actuation, approximate the solution with ON-OFF thrusters, and then iteratively linearize around the obtained solutions to improve the PWM solution. For both circular and elliptical target orbits the algorithms are simple and reasonably fast, and we showed simulations of its application favorably comparing it with an impulsive-only approach.

However, these methods are based on trajectory planning which cannot take into account orbital perturbations, disturbances or model errors. To overcome these issues, in this paper we develop a Model Predictive Control (MPC) algorithm. The term Model Predictive Control does not designate a specific control strategy but rather

⋆ The authors acknowledge financial support of the Spanish Ministry of Science and Innovation and of the European Commission for funding part of this work under grants DPI2008-05818 and EU NoE HYCON 2 (grant FP7-257462).

Peer review under responsibility of International Federation of Automatic Control.
10.1016/j.ifacol.2015.08.092

an ample range of control methods which make explicit use of a model of the process to obtain the control signal by minimizing an objective function over a finite receding horizon. In MPC the process model is used to predict the future plant outputs, based on past and current values and on the proposed optimal future control actions. These actions are calculated by the optimizer taking into account the cost function (where the fuel cost and the future tracking error are considered) as well as the constraints. The MPC algorithm developed in this paper is based on the previous open-loop PWM planner for elliptical target orbits with arbitrary eccentricity (Vazquez et al. (2014)). The MPC is initialized by first solving the open-loop problem with the PWM trajectory planning algorithm. After that, at each time step, our MPC saves time recomputing the trajectory by applying the iterative linearization scheme of the trajectory planning algorithm to the solution obtained in the previous time step.

The structure of the paper is as follows. In Section 2 we introduce the Tschauner-Hempel model, both in the impulsive and PWM case. We follow with Section 3 where we formulate the underlying optimization problems. Section 4 describes a method that solves the planning problem using PWM signals. Section 5 develops the model predictive controller. In Section 6 we show simulations of the method compared to MPC computed used an impulsive-only approach. We finish with some remarks in Section 7.

2. TSCHAUNER-HEMPEL MODEL OF SPACECRAFT RENDEZVOUS

The Tschauner-Hempel model (see Tschauner and Hempel (1965) or Carter (1998)) assumes that the target vehicle is passive and moving along an elliptical orbit with semi-major axis a and eccentricity e. Following Vazquez et al. (2014), we write the Tschauner-Hempel using eccentric anomaly instead of time. Let us first establish some notation. Note that t and E are related in a one-to-one fashion by using Kepler's equation:

$$n(t-t_p) = E - e\sin E, \tag{1}$$

where t_p is the time at periapsis, a parameter of the target's which we use as a starting point to measure the eccentric anomaly E. This equation is numerically invertible (see any Orbital Mechanics reference, such as Wie (1998)), and we will represent its inverse by the function K, i.e. $E = K(t)$. Denote by E_0 the eccentric anomaly corresponding to t_0, this is, $E_0 = K(t_0)$, and $E_k = K(t_k) = K(t_0 + kT)$, where T is an adequately chosen sampling time. Call as x_k, y_k, and z_k the position of the chaser in a local–vertical/local–horizontal (LVLH) frame of reference fixed on the center of gravity of the target vehicle at time t_k. In the (elliptical) LVLH frame, x refers to the radial position, z to the out-of-plane position (in the direction of the orbital angular momentum), and y is perpendicular to these coordinates (no longer aligned with the target velocity given that its orbit is not circular). The velocity and inputs of the chaser in the LVLH frame at time t_k are denoted, respectively, by $v_{x,k}$, $v_{y,k}$, and $v_{z,k}$, and by $u_{x,k}$, $u_{y,k}$, and $u_{z,k}$.

If there is no actuation (i.e. $u_{x,k} = u_{y,k} = u_{z,k} = 0$), the resulting transition equation was obtained exactly by Yamanaka and Ankersen (2002) as follows:

$$\mathbf{x}_{k+1} = A(t_{k+1}, t_k)\mathbf{x}_k \tag{2}$$

where

$$\mathbf{x}_k = [x_k\ y_k\ z_k\ v_{x,k}\ v_{y,k}\ v_{z,k}]^T, \tag{3}$$

and where $A(t_{k+1}, t_k) = Y_{K(t_{k+1})}Y^{-1}_{K(t_k)}$, with $Y_{K(t_k)}$ being the fundamental matrix solution of the Tschauner-Hempel model. Working expressions of this matrix and its inverse can be found in Vazquez et al. (2014). They are as in Yamanaka and Ankersen (2002) but using eccentric anomaly and a different definition of the reference axes.

Next, we formulate two versions of the discretized equations. In the first version, the control inputs are considered impulses which are applied at the middle of the sampling interval. This is referred to as the impulsive discrete model. In a second, more realistic version, thrusters can only be switched on (producing the maximum force) or off (producing no force), and only once during each sampling time. This is referred to as the PWM discrete model.

2.1 Impulsive discrete model

For the impulsive model, we assume that we can apply an impulse u in any axis and at any given sample time. For simplicity's purpose, we assume that only one impulse per axis is allowed at each time interval and model the impulse at the beginning of the time interval. We also assume that impulses are limited above and below:

$$u_{min} \leq u \leq u_{max}.$$

Exploiting the linearity of the system, it can be easily shown that

$$\mathbf{x}_{k+1} = A(t_{k+1}, t_k)\mathbf{x}_k + B(t_{k+1}, t_k)\mathbf{u}_k, \tag{4}$$

where $\mathbf{u}_k = [u_{x,k}\ u_{y,k}\ u_{z,k}]^T$ and, calling m the mass of the spacecraft (assumed constant)

$$B(t_{k+1}, t_k) = A(t_{k+1}, t_k)\begin{bmatrix} 0 & 0 & 0 \\ 0 & 0 & 0 \\ 0 & 0 & 0 \\ 1/m & 0 & 0 \\ 0 & 1/m & 0 \\ 0 & 0 & 1/m \end{bmatrix}. \tag{5}$$

Compact formulation

Next we develop a compact formulation that simplifies the notation of the problem. The state at time t_{j+k+1}, given the initial state at time t_j (which is denoted as $\mathbf{x}_j$) and the input signals from t_j to time $t_j + k$, is computed by applying recursively Equation (4) and using the fact that $A(t_{i+1}, t_i)A(t_i, t_{i-1}) = A(t_{i+1}, t_{i-1})$:

$$\mathbf{x}_{j+k+1} = A(t_{j+k+1}, t_j)\mathbf{x}_j + \sum_{i=j}^{j+k} A(t_{j+k+1}, t_{i+1})B(t_{i+1}, t_i)\mathbf{u}_i, \tag{6}$$

where it must be noted that $A(t_i, t_i) = \mathrm{Id}$, where Id is the identity matrix. Define now $\mathbf{x_S}(j)$ and $\mathbf{u_S}(j)$ as a stack of $N_p - j$ states and input signals, respectively, spanning from time t_j to time t_{N_p} for the state and from time t_{j-1} to time t_{N_p-1} for the controls, where N_p is the initial MPC horizon (and desired time of rendezvous):

$$\mathbf{x_S}(j) = \begin{bmatrix} \mathbf{x}_{j+1} \\ \vdots \\ \mathbf{x}_{N_p} \end{bmatrix}, \ \mathbf{u_S}(j) = \begin{bmatrix} \mathbf{u}_j \\ \vdots \\ \mathbf{u}_{N_p-1} \end{bmatrix}.$$

Then,

$$\mathbf{x_S}(j)=\begin{bmatrix} A(t_{j+1},t_j)\mathbf{x}_j + B(t_{j+1},t_j)\mathbf{u}_j \\ A(t_{j+2},t_j)\mathbf{x}_j + \sum_{i=j}^{j+1} A(t_{j+2},t_{i+1})B(t_{i+1},t_i)\mathbf{u}_i \\ \vdots \\ A(t_{N_p},t_j)\mathbf{x}_j + \sum_{i=j}^{N_p-1} A(t_{N_p},t_{i+1})B(t_{i+1},t_i)\mathbf{u}_i \end{bmatrix}, \quad (7)$$

which can be written as

$$\mathbf{x_S}(j) = \mathbf{F}_j\mathbf{x}_0 + \mathbf{G}_j\mathbf{u_S}, \quad (8)$$

where $\mathbf{G}_j$ is a square, block lower triangular matrix of size $N_p - j$, with its non-null elements defined by $(\mathbf{G}_j)_{kl} = A(t_{k+j}, t_{l+j})B(t_{l+j}, t_{l+j-1})$ and the matrix $\mathbf{F}_j$ is defined as:

$$\mathbf{F}_j = \begin{bmatrix} A(t_{j+1},t_j) \\ \vdots \\ A(t_{N_p},t_j) \end{bmatrix}. \quad (9)$$

2.2 PWM discrete formulation

Consider now ON-OFF thrusters with fixed force that can be only switched on or off. For simplicity, assume that there is an aligned pair of thrusters for each direction $i = 1, 2, 3$ with opposing orientation, denoted respectively as u_i^+ and u_i^-. The maximum thrust is referred to as $\bar{u}_i^+$ and $\bar{u}_i^-$, respectively. During a sample time each thruster is allowed to fire only once.

Thus, the PWM output at k is completely described by two new control variables for each pair of thrusters, as shown in Fig. 1: the pulse width $\kappa_{i,k}^+$ and the pulse start time $\tau_{i,k}^+$ (similarly $\kappa_{i,k}^-$ and $\tau_{i,k}^-$ for the negatively oriented thruster in the direction i. Then, for $t \in [kT, (k+1)T]$, we have:

$$u_i^+(t) = \begin{cases} 0, & t \in \left[kT, kT + \tau_{i,k}^+\right], \\ \bar{u}_i^+, & t \in \left[kT + \tau_{i,k}^+, kT + \tau_{i,k}^+ + \kappa_{i,k}^+\right], \\ 0, & t \in \left[kT + \tau_{i,k}^+ + \kappa_{i,k}^+, (k+1)T\right], \end{cases} \quad (10)$$

and similarly for the negatively oriented thrusters. The new control variables verify $\kappa_{i,k}^+ > 0$, $\tau_{i,k}^+ > 0$ and $\tau_{i,k}^+ + \kappa_{i,k}^+ < T$, and similarly for the negatively oriented thrusters. The last constraint prevent the PWM signal to spill over to the next time interval.

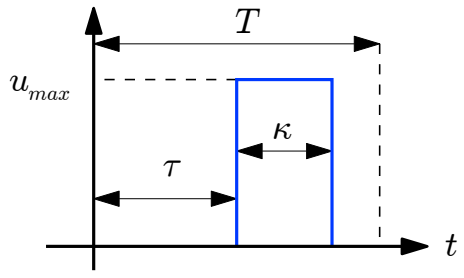

Fig. 1. PWM Variables.

Call the PWM control variables at t_k as $\mathbf{u}_k^P$:

$$\mathbf{u}_k^P = \left[\, \tau_{1,k}^+ \kappa_{1,k}^+ \tau_{1,k}^- \kappa_{1,k}^- \tau_{2,k}^+ \kappa_{2,k}^+ \tau_{2,k}^- \kappa_{2,k}^- \tau_{3,k}^+ \kappa_{3,k}^+ \tau_{3,k}^- \kappa_{3,k}^- \,\right]^T. \quad (11)$$

To find the state transition equations for PWM inputs, define, for $i = 1, 2, 3$,

$$b_i(t, \tau, \kappa) = \frac{1}{m}\int_{t+\tau}^{t+\tau+\kappa} Y_{K(s)}^{-1} C_{i+3} ds, \quad (12)$$

where C_i is a column vector of zeros with a value of one at row i. This is obtained from the variation of parameters formula for a linear inhomogeneous time-varying system. This equation can be expressed in terms of eccentric anomaly as follows:

$$b_i(t, \tau, \kappa) = \frac{1}{m}\int_{K(t+\tau)}^{K(t+\tau+\kappa)} Y_E^{-1} C_{i+3} \frac{1 - e\cos E}{n} dE. \quad (13)$$

However we cannot explicitly compute these integrals, except b_3 (see Vazquez et al. (2014)) [1] The system evolution equation for the PWM case is

$$\mathbf{x}_{k+1} = A(t_{k+1}, t_k)\mathbf{x}_k + B_{PWM}(t_{k+1}, t_k, \mathbf{u}_k^P), \quad (14)$$

where

$$B_{PWM} = \sum_{i=1}^{i=3} B_i^+ \bar{u}_i^+ + \sum_{i=1}^{i=3} B_i^- \bar{u}_i^-. \quad (15)$$

with $B_i^\pm$ column vectors defined by

$$B_i^\pm(t_{k+1}, t_k, \mathbf{u}_k^P) = Y(t_{k+1}) b_i(t, \tau_{i,k}^\pm, \kappa_{i,k}^\pm) \quad (16)$$

In this equation we need to compute b_1 and b_2 numerically.

Compact formulation
The compact formulation developed before can be readily adapted to PWM inputs. Equation (8) is now written as

$$\mathbf{x_S}(j) = \mathbf{F}_j\mathbf{x}_j + \mathbf{G}_{PWMj}(\mathbf{u_S^P}(j)), \quad (17)$$

where $\mathbf{u_S^P}(j)$ is a stack vector with all the PWM signals for j to $N_p - 1$, $\mathbf{G}_{PWMj}$ is a block lower triangular matrix with its non-null elements defined by $(\mathbf{G}_{PWMj}(\mathbf{u_S^P}(j)))_{kl} = A(t_{k+j,l+j})B_{PWM}(t_{l+j}, t_{l+j-1}, \mathbf{u}_{l+j-1}^P)$.

3. FORMULATION OF THE RENDEZVOUS PROBLEM

Next we formulate the rendezvous problem, introducing the constraints and the objective function. The formulation is done for both impulsive and PWM control signals.

3.1 Constraints on the problem

Inequality constraints on the state For sensing purposes (see e.g. Breger and How (2008)), during rendezvous it is required that the chaser vehicle remains inside a line of sight (LOS) area. To simplify the constraint, we consider a 2-D LOS area as shown in Figure 2.

For impulsive control these constraints can be formulated (see Vazquez et al. (2011) for definitions) as

$$\mathbf{A}_c\mathbf{G}\mathbf{u_S}(j) \leq \mathbf{b}_c - \mathbf{A}_c\mathbf{F}\mathbf{x}_j, \quad (18)$$

and similarly for the case of PWM control.

Equality constraints on the state

Equality constraints are formulated to ensure that the chaser spacecraft arrives at the origin with zero velocity at the end of the planning horizon. Thus, these constraints can be written as $\mathbf{x}(N_p) = \mathbf{0}$.

[1] As pointed out by a reviewer, these integrals are explicitly solved in Ankersen (2010). This will be used in future works.

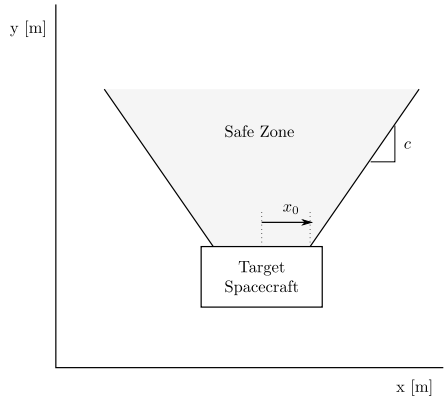

Fig. 2. Line of Sight region.

We formulate the arrival conditions as equality constraints for the control signals (see Vazquez et al. (2011) for definitions):

$$\mathbf{A}_{eq}\mathbf{G}_j\mathbf{u_S}(j) = -\mathbf{A}_{eq}\mathbf{F}_j\mathbf{x}_j, \tag{19}$$

and similarly for the case of PWM control.

Input constraints

For the case of impulsive control, we consider limitations on the magnitude of the impulses. To be able to convert the impulsive signals to PWM signals, we fix the maximum (resp. minimum) of the impulse as the maximum (resp. minus minimum) thrust of the PWM actuator times the sample time.

$$-T\bar{\mathbf{u}}^- \leq \mathbf{u_S}(j) \leq T\bar{\mathbf{u}}^+. \tag{20}$$

For the case of PWM control, the constraints are given by $\kappa_i^{\pm}(k) > 0$, $\tau_i^{\pm}(k) > 0$ and $\tau_i^{\pm}(k) + \kappa_i^{\pm}(k) < T$.

3.2 Objective function

The objective function to be minimized in the planning problem is the 1-norm of the control signal, which is proportional to fuel consumption.

Impulsive control inputs

For the case of impulsive control inputs, the objective function is given by:

$$J_{IMP}(\mathbf{u_S}(j)) = \sum_{k=j}^{N_p-1} \|\mathbf{u}_k\|_1 = \|\mathbf{u_S}(j)\|_1. \tag{21}$$

PWM control inputs

For the case of PAM control inputs, using (10) it can be seen that the objective function is given by:

$$J_{PWM}(\mathbf{u_S^P}(j)) = \sum_{k=j}^{N_p-1} \sum_{i=1}^{3} \left(\bar{u}_i^+\kappa_{i,k}^+ + \bar{u}_i^-\kappa_{i,k}^-\right). \tag{22}$$

4. THE PLANNING ALGORITHM

If we set $j = 0$ in the problem formulated in Section 3, then we are left with the planning problem of, starting at $\mathbf{x}_0$, achieving rendezvous at $k = N_p$ under the constraints. For the reader's convenience (and given it its the basis for our MPC scheme) we next summarize the planning algorithm introduced in Vazquez et al. (2014).

Step 1. The impulsive optimization problem is solved.
Step 2. The impulsive signals are converted to PWM inputs.
Step 3. The trajectory of the system with the PWM inputs is computed numerically.
Step 4. The system with PWM inputs is *linearized* around the previous step solution, thus obtaining a linear, explicit plant with respect to *increments* in the PWM inputs. Then a LP can be posed and solved to optimize the increments.
Step 5. The resulting solution is used to improve the approximation towards the real solution. Repeat the computation of Step 4 and the linearization process of Step 3 around the new solution. The process is iterated until the solution converges or time is up.

Next, we describe all the steps in our scheme.

4.1 Computation of impulsive control input

To compute the optimal control plan (with impulsive control signals), one solves

$$\begin{aligned} \min_{\mathbf{u_S}(0)} \quad & J_{IMP}(\mathbf{u_S}(0)) \\ \text{subject to: } & \mathbf{A}_c\mathbf{G}\mathbf{u_S}(0) \leq \mathbf{b}_c - \mathbf{A}_c\mathbf{F}\mathbf{x_0} \\ & \mathbf{A}_{eq}\mathbf{G}\mathbf{u_S}(0) = -\mathbf{A}_{eq}\mathbf{F}\mathbf{x}_0 \\ & -T\bar{\mathbf{u}}^- \leq \mathbf{u_S}(0) \leq T\bar{\mathbf{u}}^+. \end{aligned} \tag{23}$$

Since the cost function and the constraints are linear, then (23) can be readily solved.

4.2 Initial PWM solution: Adapting the impulsive solution

The impulsive solution from (23) is transformed to a PWM inputs, for each time instant k and direction i, as follows:

(1) Use the positive or negative thruster according to the sign of $u_{i,k}$.
(2) The pulse width has an area equal to the impulse value: $\kappa_{i,k}^{\pm} = \frac{|u_{i,k}|}{\bar{u}_i^{\pm}}$, where $\bar{u}_i^{\pm}$ is the maximum level of the (positive or negative) thruster i.
(3) Since the impulse was modeled to start at the beginning of a time sample, $\tau_{i,k}^{\pm} = 0$.

The PWM signals $\mathbf{u}_k^P$ constructed by this method produce a similar output to the system driven by impulsive signals. However, the PWM results are not necessarily optimal since their constraints are quite different; in fact, they might not even verify the constraints (as we will see in simulations). Thus, this solution is only used as an initialization for the optimization algorithm proposed next.

4.3 Computation of trajectories under PWM inputs

Next we apply (17) to compute the output of the system with PWM inputs.

4.4 Refined PWM solution: An optimization algorithm

Following Vazquez et al. (2014), we linearize B_{PWM} (using (12)–(15)) around $\mathbf{u}_k^P$. Then, we obtain

$$\begin{aligned} \mathbf{x}_{k+1} = A(t_{k+1}, t_k)\mathbf{x}_k + B_{PWM}(t_{k+1}, t_k, \mathbf{u}_k^P) \\ + B^{\Delta}(t_{k+1}, t_k, \mathbf{u}_k^P)\boldsymbol{\Delta}\mathbf{u}_k^P, \end{aligned} \tag{24}$$

where B^{Δ} can be found explicitly. The variable $\mathbf{\Delta u}_k^P$ represents the increments or decrements with respect to $\mathbf{u}_k^P$. Equation (24) becomes

$$\mathbf{x_S}(j) = \mathbf{F}_j\mathbf{x}_j + \mathbf{G}_{PWMj}(\mathbf{u_S^P}(j)) + \mathbf{G}_{\Delta j}(\mathbf{u_S^P}(j))\mathbf{\Delta_S}(j), \tag{25}$$

where $\mathbf{G}_{\Delta j}(\mathbf{u_S^P}(j))$ is a block lower triangular matrix with its non-null elements defined by

$$(\mathbf{G}_{\Delta j}(\mathbf{u_S^P}(j)))_{kl} = A(t_{k+j}, t_{l+j})B^{\Delta}(t_{l+j}, t_{l+j-1}, \mathbf{u^P_{l+j-1}}),$$

and $\mathbf{\Delta_S}(j)$ is a stack vector of the increment in the PWM variables $\mathbf{\Delta u}_k^P(j)$ from $j+1$ to N_p. The LOS constraints (18) become

$$\mathbf{A}_c\mathbf{G}_{\Delta j}\mathbf{\Delta_S}(j) \leq \mathbf{b}_c - \mathbf{A}_c\mathbf{F}\mathbf{x}_j - \mathbf{A}_c\mathbf{G}_{PWMj}, \tag{26}$$

where the dependence of $\mathbf{G_{PWM}}$ and $\mathbf{G_\Delta}$ on $\mathbf{u_S^P}$ has been omitted. Similarly, the equality constraints become:

$$\mathbf{A}_{eq}\mathbf{G}_{\Delta j}\mathbf{\Delta_S}(j) = -\mathbf{A}_{eq}\mathbf{F}_j\mathbf{x}_j - \mathbf{A}_{eq}\mathbf{G}_{PWMj}. \tag{27}$$

The constraints on the $\mathbf{\Delta u}_k^P$ are as follows:

$$-\Delta\kappa_i^{\pm}(k) \leq \kappa_i^{\pm}(k),\ -\Delta\tau_i^{\pm}(k) \leq \tau_i^{\pm}(k) \tag{28}$$

$$\Delta\tau_i^{\pm}(k) + \Delta\kappa_i^{\pm}(k) \leq T - \tau_i^{\pm}(k) - \kappa_i^{\pm}(k), \tag{29}$$

$$|\mathbf{\Delta u}_k^P| \leq \mathbf{\Delta}^{MAX}, \tag{30}$$

for $k = j$ up to $k = N_p - 1$, where (30) is used to avoid large variations that might make the linearization approximation to fail. These constraints are summarized as $\mathbf{A_\Delta}(k)\mathbf{\Delta_S}(k) \leq \mathbf{b_\Delta}(k)$. Finally, the objective function can be rewritten in terms of $\mathbf{\Delta_S}(j)$ as $J(\mathbf{u_S^P}(j), \mathbf{\Delta_S}(j)) = J_{PWM}(\mathbf{u_S^P}(j)) + J^{\Delta}(\mathbf{\Delta_S}(j))$, where

$$J^{\Delta}(\mathbf{\Delta_S(j)}) = \sum_{k=j}^{N_p-1}\sum_{i=1}^{3}\left(\bar{u}_i^+\Delta\kappa_{i,k}^+ + \bar{u}_i^-\Delta\kappa_{i,k}^-\right). \tag{31}$$

Thus, for the planning problem an LP with PWM outputs can be posed as follows:

$$\min_{\mathbf{\Delta_S}(0)} \quad J^{\Delta}(\mathbf{\Delta_S}(0)) \tag{32}$$

$$\begin{aligned}\text{s. t.: } \mathbf{A}_c\mathbf{G}_{\Delta 0}\mathbf{\Delta_S}(0) &\leq \mathbf{b}_c - \mathbf{A}_c\mathbf{F}_0\mathbf{x}_0 - \mathbf{A}_c\mathbf{G}_{PWM0},\\ \mathbf{A}_{eq}\mathbf{G}_{\Delta 0}\mathbf{\Delta_S}(0) &= -\mathbf{A}_{eq}\mathbf{F}_0\mathbf{x}_0 - \mathbf{A}_{eq}\mathbf{G}_{PWM0},\\ \mathbf{A_\Delta}\mathbf{\Delta_S}(0) &\leq \mathbf{b_\Delta}.\end{aligned}$$

The solution $\mathbf{\Delta_S}(0)$ is used to recompute new PWM inputs, $\mathbf{u_S^{P^{NEW}}}(0) = \mathbf{u_S^P}(0) + \mathbf{\Delta_S}(0)$. Then $\mathbf{u_S^{P^{NEW}}}(0)$ is used to recompute the matrices in (33), including $\mathbf{G}_{PWM0}$, and the optimization problem is solved again. The procedure is iterated until there is convergence.

5. MODEL PREDICTIVE CONTROL

Trajectory planning cannot take into account orbital perturbations, disturbances or model errors. To overcome these issues, we need closed-loop control. In particular, model predictive control closes the loop by simply re-planning the maneuver at each time step after applying just one set of control inputs. The re-planning is done from the actual position at each time step, which seldom coincides with the planned position due to disturbances.

However, it is not necessary to repeat all the steps of Section 4. Since the new position should be close to the planned one, we can apply the linearization scheme of the planning algorithm starting from the last available linearization. We summarize the MPC algorithm next:

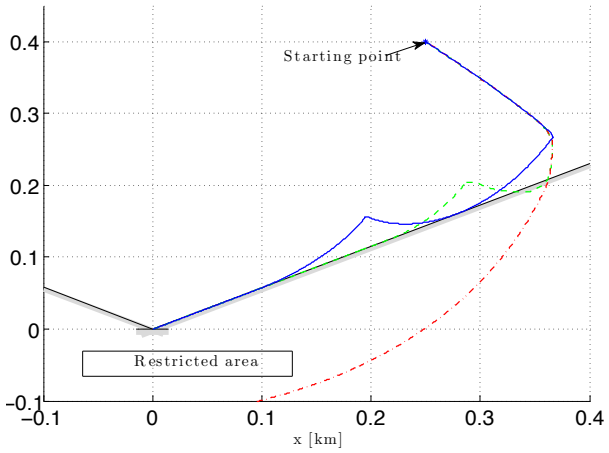

Fig. 3. System trajectories in the target orbital plane: open-loop PWM inputs computed from impulsive solution (dot-dashed), closed-loop Model Predictive Control with PWM inputs using impulsive model (dashed), and closed-loop Model Predictive Control with PWM inputs using the PWM planning algorithm (solid).

Step 1. At time step $j = 0$ and starting from $\mathbf{x}_0$ apply the Planning algorithm of Section 4, obtaining a set of impulses $\mathbf{u_S^P}(0)$ that would guarantee rendezvous if there were no disturbances.
Step 2. Apply impulses corresponding to the first time instant; save the rest of impulses, $\mathbf{u_S^P}(1)$. Set $j = 1$
Step 3. One arrives at $\mathbf{x}_j$, which probably is not the intended value of the state at time j but close.
Step 4. Apply the linearization algorithm of Section 4.4 using the previous impulses $\mathbf{u_S^P}(j)$ as initial guess to obtain a new set of impulses $\mathbf{u_S^P}(j)$. Apply the impulses corresponding to time j.
Step 5. Repeat 3 until $j = N_p$ (rendezvous).

The optimization problem to be solved in Step 3 is

$$\min_{\mathbf{\Delta_S}(j)} \quad J^{\Delta}(\mathbf{\Delta_S}(j)) \tag{33}$$

$$\begin{aligned}\text{s. t.: } \mathbf{A}_c\mathbf{G}_{\Delta j}\mathbf{\Delta_S}(j) &\leq \mathbf{b}_c - \mathbf{A}_c\mathbf{F}_j\mathbf{x}_j - \mathbf{A}_c\mathbf{G}_{PWMj},\\ \mathbf{A}_{eq}\mathbf{G}_{\Delta j}\mathbf{\Delta_S}(j) &= -\mathbf{A}_{eq}\mathbf{F}_j\mathbf{x}_j - \mathbf{A}_{eq}\mathbf{G}_{PWMj},\\ \mathbf{A_\Delta}\mathbf{\Delta_S}(j) &\leq \mathbf{b_\Delta}.\end{aligned}$$

The solution $\mathbf{\Delta_S}(j)$ is used to recompute new PWM inputs, $\mathbf{u_S^{P^{NEW}}}(j) = \mathbf{u_S^P}(j) + \mathbf{\Delta_S}(j)$, and the procedure is iterated until it converges or time is up.

6. SIMULATION RESULTS

For simulations we choose $N_p = 50$ as planning horizon, $T = 60$ s, and $\bar{u} = 10^{-1}$ N/kg. The target orbit has $e = 0.7$ and perigee altitude $h_p = 500$ km. Initial conditions were $\theta_0 = 45^{\text{o}}$, $\mathbf{r}_0 = [0.25\ 0.4\ -0.2]^T$ km, $\mathbf{v}_0 = [0.005\ -0.005\ -0.005]^T$ km/s. The LOS constraint (see Vazquez et al. (2011)) is defined by $x_0 = 0.001$ km and $C_{LOS} = \tan 30^{\text{o}}$.

In the simulations four algorithms were considered: first, an impulsive open-loop trajectory planner, as described in Section 4.1. Next, the full PWM planner of Section 4. Next, closed-loop simulations using MPC, based either on the impulsive planner, or on the full PWM algorithms as explained in Section 5. The impulses produced by the first and third methods are subsequently transformed to PWM inputs using the algorithm of Section 4.2.

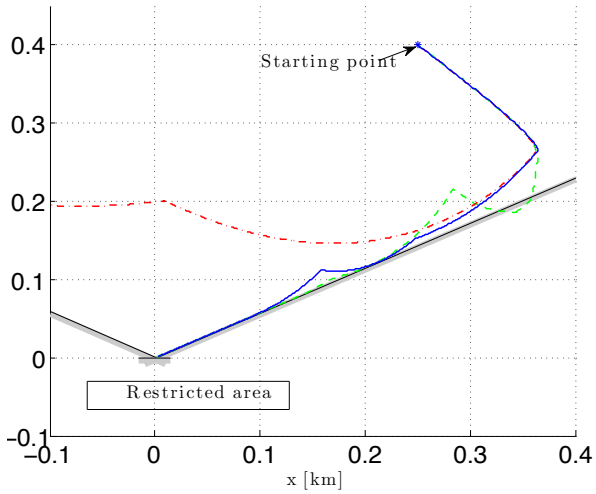

Fig. 4. System trajectories in the target orbital plane, with inexact thruster model: open-loop PWM inputs computed with the planning algorithm (dot-dashed), closed-loop Model Predictive Control with PWM inputs using impulsive model (dashed), and closed-loop Model Predictive Control with PWM inputs using the PWM planning algorithm (solid).

We first compare the algorithms without disturbances. The trajectories (projected on the target orbital plane) are shown in Fig. 3. The open-loop impulsive solution does not achieve rendezvous and drifts away, whereas the other solutions successfully reach the origin. The impulsive MPC is able to compensate its imperfect thruster model, without violating the constraints. There was no visible difference between the open-loop and the MPC closed loop PWM algorithms. The cost for the impulsive solution was 14.6 m/s, while the PWM planner had a cost of 15.2 m/s (MPC was able to reduce it slightly to 15.1 m/s) whereas the impulsive MPC had a cost of 15.7 m/s.

Next in Fig. 4 we show a simulation where the maximum and minimum thrust is not perfectly calibrated (with biases of about 1-3% for each thruster). Now, the open-loop PWM planner fails to achieve rendezvous, whereas both MPC algorithms reach the origin. The impulsive MPC, however, slightly exists the line-of-sight region. The cost for the PWM MPC algorith was 15.1 m/s, whereas the impulsive MPC had a cost of 15.8 m/s.

Each iteration took less than 1s on a conventional computer, using MATLAB and the *Gurobi* optimization package (see Gurobi Optimization, Inc. (2014)). With a maximum number of iterations of 6, the computation time remained well below the interval sampling time.

7. CONCLUDING REMARKS

We have presented a MPC algorithm that computes optimal PWM inputs for the problem of rendezvous in elliptical orbits. The algorithm might be particularly useful for satellites with small specific thrust. The algorithm improves the results of an impulsive-only MPC (with the impulses posteriorly transformed to PWM inputs), particularly in the presence of disturbances, which would help avoiding a PWM approximation term typically included in the "uncertainty budget" for robust design. Inclusion of real-life constraints and more realistic simulations are needed to validate the method.

REFERENCES

Ankersen, F. (2010). *Guidance, Navigation, Control and Relative Dynamics for Spacecraft Proximity Maneuvers*. Ph.D. thesis.

Arzelier, D., Kara-Zaitri, M., Louembet, C., and Delibasi, A. (2011). Using polynomial optimization to solve the fuel-optimal linear impulsive rendezvous problem. *J. Guid. Contr. Dynam.*, 34, 1567–1572.

Arzelier, D., Louembet, C., Rondepierre, A., and Kara-Zaitri, M. (2013). A new mixed iterative algorithm to solve the fuel-optimal linear impulsive rendezvous problem. *J. Opt. Theor. Appl.*, 159, 210–230.

Asawa, S., Nagashio, T., and Kida, T. (2006). Formation flight of spacecraft in earth orbit via MPC. In *SICE-ICASE International Join Conference*.

Breger, L. and How, J.P. (2008). Safe trajectories for autonomous rendezvous of spacecraft. *J. Guid. Contr. Dynam.*, 31(5), 1478–1489.

Carter, T.E. (1998). State transition matrices for terminal rendezvous studies: Brief survey and new example. *J. Guid. Contr. Dynam.*, 21(1), 148–155.

Clohessy, W.H. and Wiltshire, R.S. (1960). Terminal guidance systems for satellite rendezvous. *J. Aerosp. Sc.*, 27(9), 653–658.

Gavilan, F., Vazquez, R., and Camacho, E.F. (2009). Robust model predictive control for spacecraft rendezvous with online prediction of disturbance bound. In *Proceedings of AGNFCS'09, Samara, Russia,*.

Gavilan, F., Vazquez, R., and Camacho, E.F. (2012). Chance-constrained model predictive control for spacecraft rendezvous with disturbance estimation. *Contr. Eng. Pract.*, 20(2), 111–122.

Gurobi Optimization, Inc. (2014). Gurobi optimizer reference manual. URL `http://www.gurobi.com`.

Hartley, E.N., Trodden, P.A., Richards, A.G., and Maciejowski, J.M. (2012). Model predictive control system design and implementation for spacecraft rendezvous. *Control Engineering Practice*, 20(7), 695 – 713.

Larsson, R., Berge, S., Bodin, P., and Jönsson, U. (2006). Fuel efficient relative orbit control strategies for formation flying and rendezvous within prisma. In *Proceedings of the 29th AAS guidance and control conference*.

Leomanni, M., Rogers, E., and Gabriel, S.B. (2014). Explicit model predictive control approach for low-thrust spacecraft proximity operations. *Journal of Guidance, Control, and Dynamics*, 37(6), 1780–1790.

Richards, A.G. and How, J. (2003). Performance evaluation of rendezvous using model predictive control. AIAA Paper 2003-5507.

Rossi, M. and Lovera, M. (2002). A multirate predictive approach to orbit control of small spacecraft. In *Proceedings of ACC 2002*.

Tschauner, J. and Hempel, P. (1965). Rendevous zu einem in elliptischer bahn umlaufenden. *Ziel. Acta Astronaut.*, II(2), 104–109.

Vazquez, R., Gavilan, F., and Camacho, E.F. (2014). Trajectory planning for spacecraft rendezvous in elliptical orbits with On/Off thrusters. In *IFAC World Congress, Cape Town*.

Vazquez, R., Gavilan, F., and Camacho, E.F. (2011). Trajectory planning for spacecraft rendezvous with on/off thrusters. In *Proc. of IFAC World Congress 2011*.

Wie, B. (1998). *Space vehicle dynamics and control*. AIAA.

Yamanaka, K. and Ankersen, F. (2002). New state transition matrix for relative motion on an arbitrary elliptical orbit. *J. Guid. Contr. Dynam.*, 25(1), 60–66.